

Preparation and microwave properties of Ni hollow fiber by electroless plating-template method

Haijun Zhang*, Yun Liu

High Temperature Ceramics Institute, Zhengzhou University, 75 Daxue Road, Zhengzhou, Henan Province 450052, PR China

Received 8 February 2007; received in revised form 29 April 2007; accepted 5 May 2007

Available online 10 May 2007

Abstract

Nickel-coated silk composites (Ni/silk fiber) were prepared by electroless nickel-plating using a kind of natural silk as template in first stage. The silk templates were then removed to get Ni hollow fiber by annealing the Ni/silk fiber at 220 °C for 2 h in air or 700 °C for 1.5 h in nitrogen. The prepared Ni/silk fiber and Ni hollow fiber were characterized by X-ray diffraction (XRD), scanning electron microscope (SEM), field emission scanning electron microscope (FE-SEM) and differential thermal analysis and thermogravimetric analysis (TG-DTA). The values of complex permittivity, complex permeability, dielectric and magnetic loss of Ni/silk fiber and Ni hollow fiber were measured in the frequency range of 2–18 GHz by a reflection/transmission approach using a network analyzer. The results indicate that the dielectric loss of Ni/silk fiber and Ni hollow fiber is high up to 1 even at 18 GHz while the magnetic loss is low.

© 2007 Elsevier B.V. All rights reserved.

Keywords: Metals and alloys; Chemical synthesis; Dielectric response; Magnetisation; Scanning electron microscopy

1. Introduction

Metal fiber is a kind of very important potential candidate for radar adsorbing materials (RAM) [1–2]. A great deal of work has been done on both flaky and spherical magnetic metal particles. The results showed that those particles exhibited magnetic losses in the microwave frequency range, and their microwave permeability depended on particle size [3–8]. However, there have been few studies of the microwave characteristics of magnetic metal fiber. Generally speaking, the methods of bundle-drawing, melt-extraction and chatter-machining [9–13] can be used for production of metal fiber more than 10 μm. However, it is very difficult to get hollow metal fiber with the above-mentioned methods. As a matter of fact, using as RAM, metal hollow fiber seems to be better than metal solid fiber in terms of its lower weight.

Electroless plating is widely used in many fields for its advantages, such as low cost, easy formation of a continuous and uniform coating on the surface of substrate with complex shape

and capability of depositing on either conductive or nonconductive substrates. Recently, electroless plating has also attracted a lot of interests in preparation of low dimensional nanostructured material [14–19] and in the decoration on carbon nanotubes, SiC ultrafine powder, etc. [17,20–24].

Although electroless plating routes have been previously used to produce various composite powders with multiple components and coatings, metal hollow fiber prepared by these routes has not been previously reported. And to the knowledge of the authors, the microwave properties of hollow nickel fiber have not been previously reported yet. This paper reports our results on preparation and microstructure of Ni hollow fiber by an electroless plating and template removing method. The complex permittivity and permeability of Ni hollow fiber in 2–18 GHz were also investigated.

2. Experimental procedure

A kind of natural silk was used as template to prepare nickel-coated silk composites (Ni/silk fiber). The original average length of the starting silk is more than 300 μm, as shown in Fig. 1 indicating that the surface of the starting silk is very smooth. The original silk was cut into pieces with a length of about 50–100 μm for electroless plating.

Surface treatment of the natural silk was carried out before electroless plating in order to get complete, continuous nickel film. First, the natural silk was

* Corresponding author. Tel.: +86 371 67761908; fax: +86 371 67763822.

E-mail addresses: zhanghaijun@zzu.edu.cn, zhjzdl@yahoo.com.cn (H. Zhang).

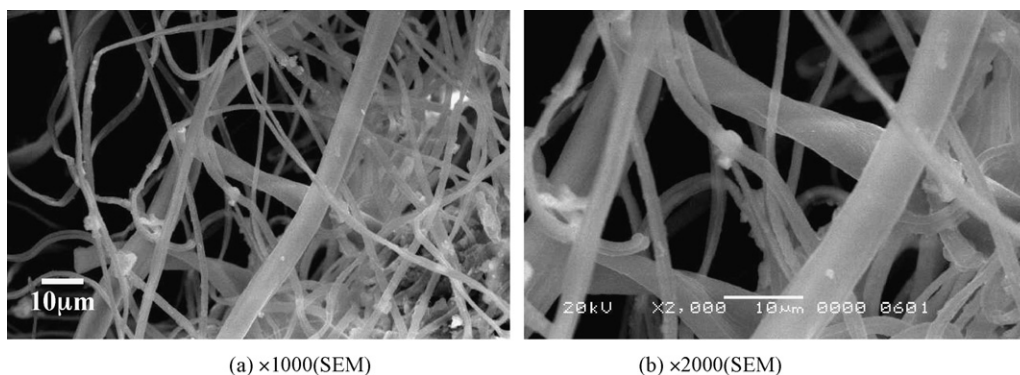


Fig. 1. SEM photograph of natural surface of silk.

immersed in acetone and then in HF (aq) with ultrasonic vibration for 15 min. After that, the cleaned natural silk was sensitized in a mixed solution of stannous chloride ($\text{SnCl}_2 \cdot \text{H}_2\text{O}$) and hydrochloric acid (HCl) solution for 1 h and then activated in palladium chloride (PdCl_2) and hydrochloric acid for another 1 h.

Solution of nickel ion was prepared by dissolving an analytical grade $\text{NiSO}_4 \cdot 6\text{H}_2\text{O}$ in distilled water. The pH values of the solution was adjusted by sodium carbonate solution to 10.7 and the solution was heated to 80 °C. Cetyltrimethyl ammonium bromide (CTMAB) was chosen as surfactant, with sodium citrate ($\text{Na}_3(\text{Cit})$) as the complex agent, and hydrazine hydrate as the reducing agent. Electroless nickel-plating solution was prepared by adding the following components in the following order:

$\text{NiSO}_4 \cdot 6\text{H}_2\text{O}$	0.25 mol/L
$\text{Na}_3(\text{Cit})$	0.0625 mol/L
CTMAB	0.5 wt.% relative to starting natural silk
Hydrazine hydrate	0.75 mol/L

The silk was placed in nickel solution for 2 h. Then the mixture composites were separated from the solution by filtration separation, washed with distilled water, ethanol and acetone respectively, and dried at 60 °C for 12 h. Gray-black Ni-coated silk composites were obtained. The Ni-coated silk composite was annealed in air (or nitrogen) atmosphere to remove the silk template, and to get the Ni hollow fiber.

To compare the micrograph of pure nickel powder with that of the Ni/silk fiber, pure nickel powders were also prepared from NiSO_4 aqueous solution by electroless plating method using hydrazine hydrate as reductant. The principal factors of pure ultrafine Ni powder synthesis are as follows: pH value of bathing solution is 10.7; bathing temperature is 80 °C; molar ratio of $[\text{N}_2\text{H}_4 \cdot \text{H}_2\text{O}]/[\text{Ni}^{2+}]$

is 3.0; the concentration of $[\text{Ni}^{2+}]$ is 0.25 M; the molar ratio of $[\text{Na}_3(\text{Cit})]/[\text{Ni}^{2+}]$ is 1:4; the bathing time is 2 h; the amount of CTMAB is 0.5 wt.% relative to final ultrafine nickel powders.

Differential thermal analysis coupled with thermogravimetric analysis of the Ni-coated silk composites was carried out on a NETZSCH STA-449C Thermal Analysis System with a heating temperature rate of 10 °C/min in flowing air. The sample pot was platinum, and the reference material was α -alumina.

The XRD data were collected by PHILIPS diffractometer (Model X'Pert PRO, Cu K α radiation, 40 kV, 40 mA) in the 2θ ranging from 30° to 80° with a step width of 0.016°. The apparent crystallite size of the coated nickel was determined using the Scherrer formula.

Fiber morphology was characterized via scanning electron microscopy (SEM) (Model, JSM-5610LV, JEOL, JAPAN, 20 kV) coupled with EDS (Model, Oxford 6587, England) and field emission scanning electron microscopy (FE-SEM) (Model, JSM-6700F, JEOL, JAPAN, 15 kV). The fiber was ultrasonically dispersed into water, and the resultant suspension was spread on the surface of a polished silicon plate. The samples were coated with a thin layer of platinum for conductivity before SEM and FE-SEM observation.

Ni/silk fiber–paraffin wax and the Ni hollow fiber–paraffin wax composites were prepared by homogeneously mixing the fiber with paraffin wax (with about 20% of fiber by volume). Toroidal-shaped samples with an inner diameter of 3.02 mm, an outer diameter of 7.0 mm and a length of 3–4 mm were prepared. A network analyzer (Agilent PNA N5230A Network Analyzers) was employed to measure reflected and transmitted scattering parameters (S_{11} , S_{21}) and determine the values of ϵ' , ϵ'' , μ' and μ'' of Ni/silk fiber and Ni hollow fiber in the frequency range of 2–18 GHz by using a reflection/transmission technique [25,26].

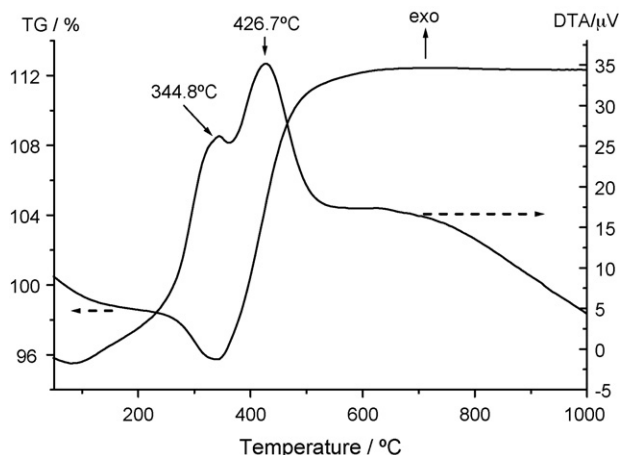


Fig. 2. Differential thermal analysis and thermogravimetric of Ni/silk in air.

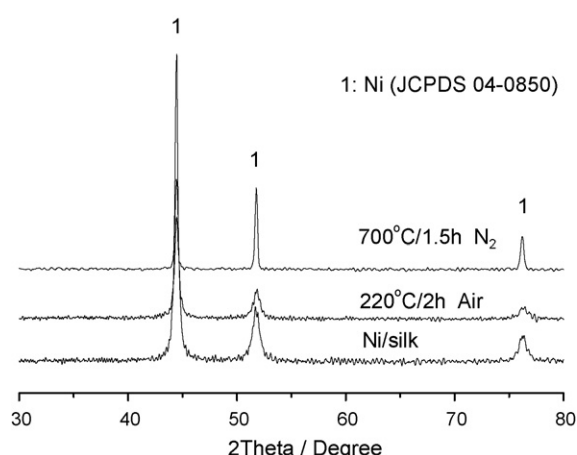
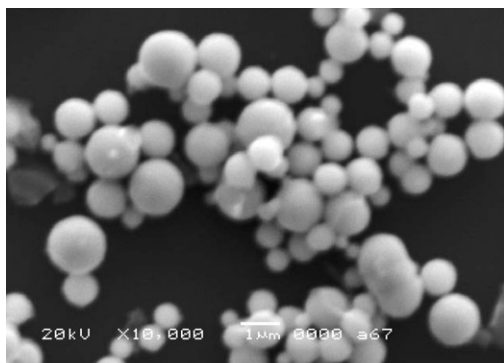
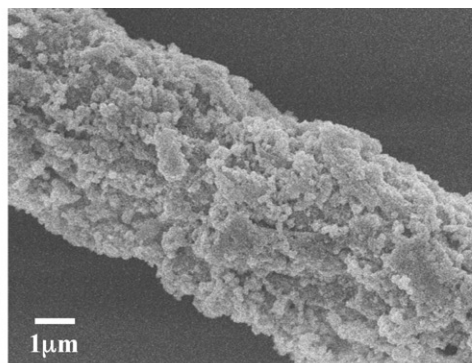


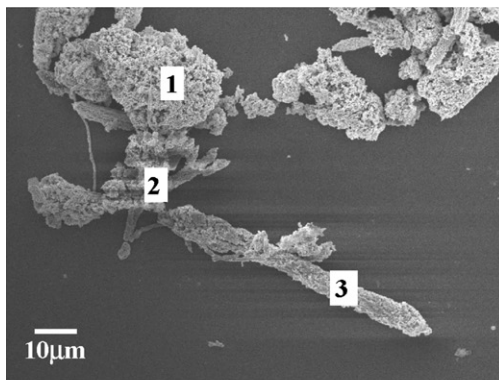
Fig. 3. XRD results of Ni/silk, Ni/silk annealed in air and nitrogen.



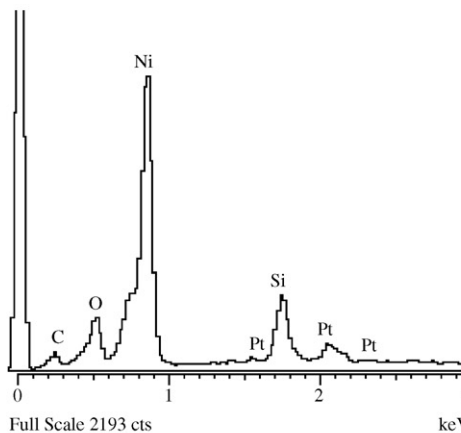
(a) nickel powders, ×10000(SEM)



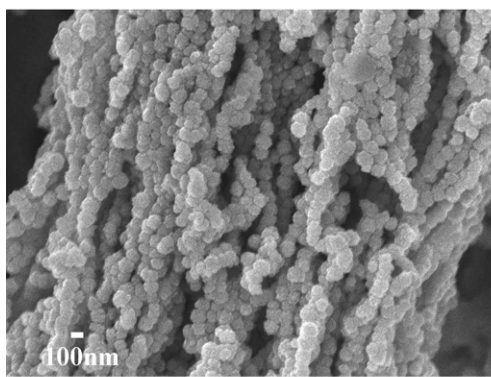
(b) Ni/silk, ×10000(FESEM)



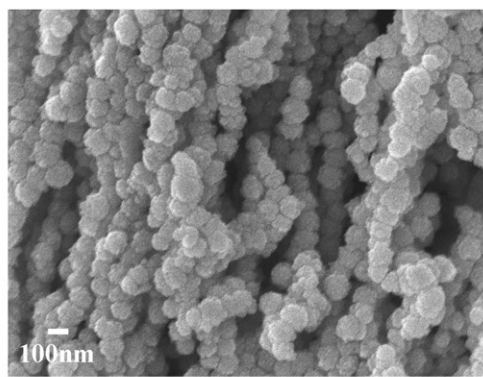
(c) Ni/silk, ×1000(FESEM)



(d) Ni/silk, EDS of point 3 in Fig.4c



(e) Ni/silk, ×30000(FESEM)



(f) Ni/silk, ×50000(FESEM)

Fig. 4. SEM (FE-SEM) photograph of Ni/silk and nickel powders by electroless plating.

Table 1
The EDS results of Ni/silk fiber in Fig. 4c

Spectrum	C	O	Si	Ni	Total
Spectrum 1	5.95	2.24	3.99	87.82	100.00
Spectrum 2	9.53	3.13	38.89	48.45	100.00
Spectrum 3	4.52	1.22	31.64	62.62	100.00
Mean	6.67	2.20	24.84	66.30	

All results in weight percent.

Table 2
The EDS results of Ni hollow fiber in Fig. 5a

Spectrum	O	Si	Ni	Total
Spectrum 1	2.00	1.36	96.64	100.00
Spectrum 2	1.85	1.93	96.21	100.00
Spectrum 3	1.72	1.46	96.81	100.00
Spectrum 4	0.00	0.87	99.13	100.00
Spectrum 5	2.17	1.01	96.82	100.00
Mean	1.55	1.33	97.12	100.00

All results in weight percent.

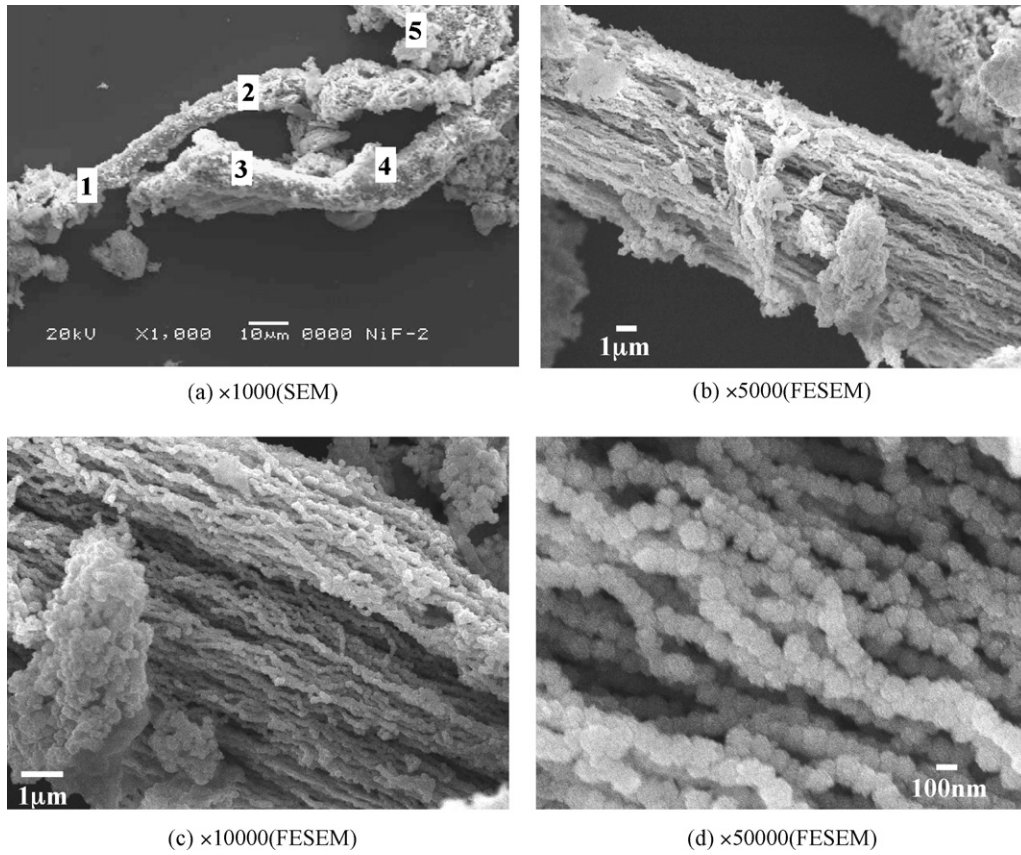


Fig. 5. SEM (FE-SEM) photograph of Ni hollow fiber annealed at 210 °C for 2 h in air.

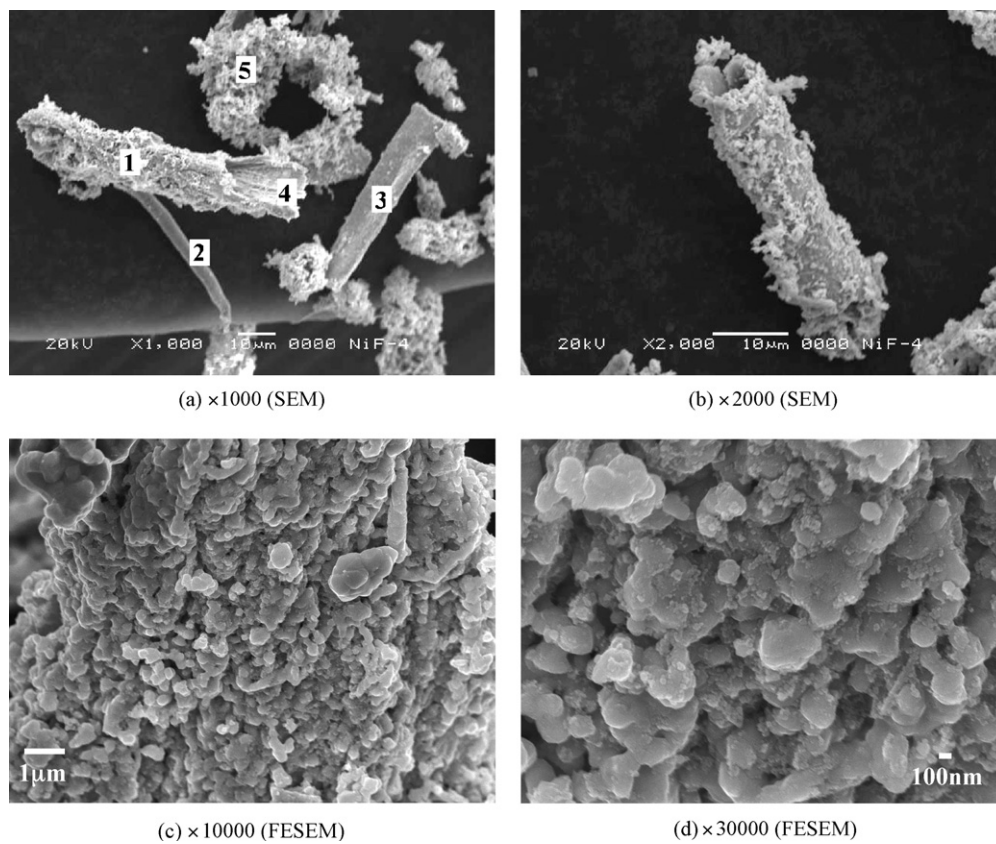


Fig. 6. SEM (FE-SEM) photograph of Ni hollow fiber annealed at 700 °C for 1.5 h in nitrogen.

3. Results and discussions

The TG-DTA curves of the prepared Ni/silk fiber in air were shown in Fig. 2. The results indicated that the weight change could be divided into two temperature regions, namely, from room temperature (RT) to about 340 °C with a weight loss of about 5% and from 340 to 500 °C with a weight increase of about 12% to initial weight. At temperature higher than 500 °C, there was almost no change in weight increase that can be attributed to the formation of a pure oxide system (NiO). In the temperature region from RT to about 340 °C, the weight loss can be ascribed to the oxidation of the template silk playing the main role. The weight gain in 340–500 °C might result from the oxidation of the coated nickel. Based on the above results, the Ni-coated silk composite was annealed at 220 °C for 2 h in air (or at 700 °C for 1.5 h in nitrogen atmosphere) in order to avoid the oxidation of the coated nickel and obtain Ni hollow fiber.

It is seen from Fig. 3 that only pure Ni was present in all samples of original Ni/silk fiber, and the Ni/silk fiber annealed in air and nitrogen, and the crystalline size of coated nickel was about 20–30 nm as determined by the XRD line-broadening technique. These results indicate that nickel was coated on the surface of the natural silk, and no oxidation of the coated nickel occurred during the heat treatment process either in air or in nitrogen. All the nickel diffraction peaks of Ni/silk fiber heated in nitrogen became much sharper than those of the original sample, implying that the crystalline size of the sample was increased during high temperature heat treatment in nitrogen.

Fig. 4 shows SEM morphology of natural surface of pure nickel powders and Ni/silk fiber prepared by electroless plating. It is seen that these pure Ni particles possess global structures with diameters of about 0.5–1.5 μm (Fig. 4a). However, the particle is congregated together, which can be attributed to the nickel's magnetic attractive force. Fig. 4b shows the typical morphology of the Ni/silk fiber by electroless plating. Comparing Fig. 4b with Fig. 1 (the morphology of the starting silk) reveals that the surface of Ni/silk fiber is much rougher than that of the starting silk demonstrating that some new phases formed on the surface of starting silk. Fig. 4c shows that the formed Ni/silk fiber has several different shapes. Some fiber interweave each other and form sphere-like structure (as shown in point 1, Fig. 4c), some fiber form a spiral-like structure (point 2, Fig. 4c) and some silk keep the starting original shape of the template with a length of about 70 μm (point 3, Fig. 4c). Fig. 4d and Table 1 shows that elements Ni, C, Si and O are found in Ni/silk

Table 3
The EDS results of Ni hollow fiber in Fig. 6a

Spectrum	Si	Ni	Total
Spectrum 1	0.52	99.48	100.00
Spectrum 2	0.39	99.61	100.00
Spectrum 3	0.00	100.00	100.00
Spectrum 4	0.65	99.35	100.00
Spectrum 5	0.74	99.26	100.00
Mean	0.46	99.54	100.00

All results in weight percent.

fiber. Ni element resulted from the electroless plating and C element from the starting silk. The observed silicon element can be ascribed to the silicon plate bearing the composite powder, and the oxygen element may be due to little oxidation of coated nickel. These results confirm that the prepared fiber was Ni/silk fiber. Comparing Ni/silk fiber (Fig. 4e and f) with the starting silk (Fig. 1) shows that the surface of Ni/silk fiber is uneven and composed of small particles with size less than 100 nm (Fig. 4f) and Ni nanocrystals are arrayed nearly parallel to the axes of the starting silk (Fig. 4e and f). It can be seen by comparing Fig. 4e and f with Fig. 4a that the morphologies of coated Ni on the surface of Ni/silk fiber are also different from the pure Ni particles by electroless plating as the size of coated Ni on the surface of Ni/silk fiber is much smaller than that of the pure nickel. The result suggests that the presence of the silk template impedes the grain-boundary movement of the coated nickel and plays a role in preventing grain-growth.

Fig. 5 shows morphology of the Ni hollow fiber annealed at 220 °C for 2 h in air. Compared Fig. 5 with Fig. 4b, it can be seen that the surface of the Ni hollow fiber is much more porous than that of the Ni/silk fiber, and there exists a large number of

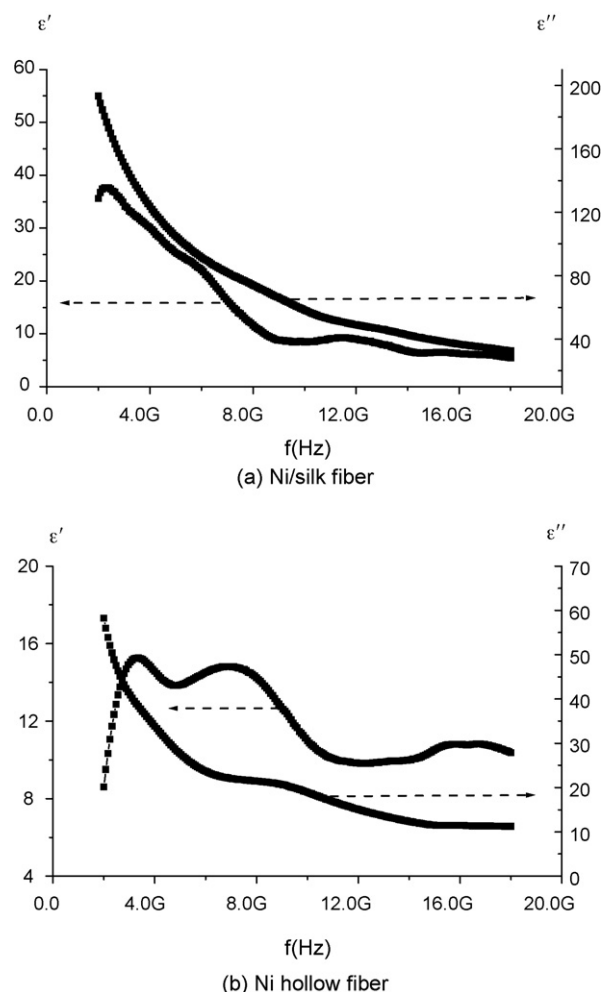


Fig. 7. Frequency dependence of complex permittivity of ultrafine Ni/silk fiber and Ni hollow fiber (heat treatment in nitrogen at 700 °C for 1.5 h)–paraffin wax composites.

small pores on the surface of Ni hollow fiber due to oxidation of the silk and removal of the CO and CO₂ gas. The Ni hollow fiber is composed of parallel nanowires, which are arrayed along the axis of the starting silk. The nanowires also consisted of the nickel particles with size of less than 100 nm, which is almost the same as that of the Ni/silk fiber indicating that the nano-sized Ni particles do not grow much at 220 °C for 2 h. The EDS results (Table 2) of the Ni hollow fiber in Fig. 5a shows that the elements Ni, Si and O are found in the samples. The observed silicon element is ascribed to the silicon plate bearing composite powder, and the little amount of oxygen element may be due to partial oxidation of coated nickel. The absence of carbon element indicates that all the silk is removed during the heat treatment process.

Fig. 6 exhibits particle morphology of the Ni hollow fiber heated at 700 °C for 1.5 h in nitrogen. The fracture section of the fiber in Fig. 6a and b confirms that the hollow fiber is formed. Comparing Fig. 6c and d with Fig. 5c and d reveals that no nanowire was formed for the samples annealed in nitrogen, and the particle size of nickel in the sample heated in nitrogen is much larger than that of the sample annealed in air, which can be ascribed to the much higher temperature used for the sample fired in nitrogen. It is seen from Table 3 (the EDS results of the fiber in Fig. 6a) that only the elements Ni and Si are found. All

the results demonstrate that Ni hollow fiber is prepared in this work.

Fig. 7 shows the frequency dependence of complex permittivity of Ni/silk fiber and Ni hollow fiber (annealed at 700 °C for 1.5 h in nitrogen) in 2–18 GHz. It indicates:

- (1) For Ni/silk fiber, ϵ' and ϵ'' decreases with measuring frequency increasing, the value of ϵ'' at low frequency is as high as 200, and it possesses a value of about 40 even at 18 GHz.
- (2) For Ni hollow fiber, ϵ'' decreases with measuring frequency increasing, the values of ϵ'' at low frequency are as high as 60, and it keeps a value of about 10 even at 18 GHz. The value of ϵ' increases with frequency up to about 4 GHz, after that, it decreases; the value of ϵ' at 18 GHz is about 10.
- (3) The values of ϵ' and ϵ'' of Ni/silk fiber are much higher than that of the Ni hollow fiber. The reason for this difference needs further investigation.

Fig. 8 shows that μ' had the value 1.0 more or less in all measuring frequencies for both Ni/silk and Ni hollow fiber, and no resonance peaks is observed in the μ'' spectrum. It is due to the microwave magnetic loss of magnetic materials originates mainly from domain wall resonance and natural ferromagnetic resonance. The domain wall resonance occurs only in

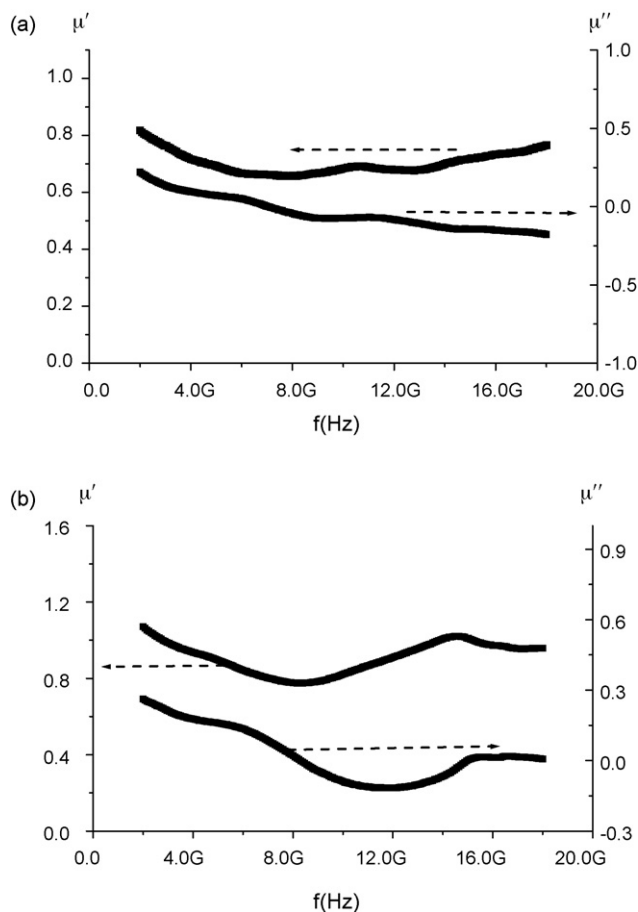


Fig. 8. Frequency dependence of complex permeability of ultrafine Ni/silk fiber and Ni hollow fiber (heat treatment in nitrogen at 700 °C for 1.5 h)–paraffin wax composites.

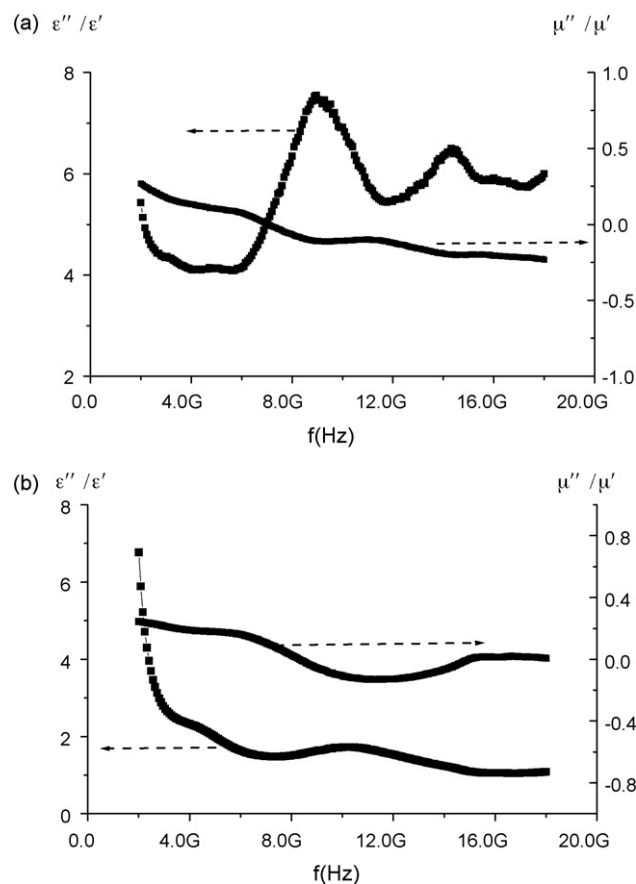


Fig. 9. Frequency dependence of dielectric and magnetic loss of ultrafine Ni/silk fiber and Ni hollow fiber (heat treatment in nitrogen at 700 °C for 1.5 h)–paraffin wax composites.

multidomain materials and usually in the 1–100 MHz range. And it has been reported that the natural resonance frequency for Ni particles ($d_m = 1.4 \mu\text{m}$) is about 1.8 GHz [27]. In this study, the permeabilities were measured in frequency range of 2–18 GHz, so neither domain wall resonance nor natural ferromagnetic resonance is observed. The value of μ'' is relatively low and the maximum value is no more than 0.3 in all 2–18 GHz.

Fig. 9 shows the frequency dependence of dielectric loss and magnetic loss in 2–18 GHz for Ni/silk fiber and Ni hollow fiber–paraffin wax composites. It indicates that:

- (1) For Ni/silk fiber, the dielectric loss is observed to be very high with values of more than 4 in all frequencies. However, the magnetic loss of Ni fiber–paraffin wax composites is low with values of about 0.1–0.2 in 2–18 GHz. Two dielectric loss peaks is observed in the range of 2–18 GHz, and the corresponding frequency is about 8.96 and 14.48 GHz. The maximum dielectric loss measured is up to 7.6.
- (2) For Ni hollow fiber, the dielectric loss decreases with frequency increasing, and its value is observed to be high up to 7 at 2 GHz and about 1 even at 18 GHz. However, the magnetic loss of Ni hollow fiber is close to that of Ni/silk fiber.
- (3) The particular high dielectric loss of both Ni/silk and Ni hollow fiber may be due to the anisotropy of the prepared Ni fiber. The reason of the different behavior of $(\epsilon''/\epsilon)-f$ curve of Ni/silk fiber and Ni hollow fiber may be due to the obvious different crystalline size of those two kinds of fiber.

4. Conclusions

Ni hollow fiber was prepared by electroless plating and template removing process using hydrazine hydrate, NiSO_4 , a kind of natural silk, etc. as starting materials. Heat treatment at 220°C for 2 h in air or at 700°C for 1.5 h in nitrogen atmosphere was suitable for removing the starting silk template. The typical length of the Ni hollow fiber was about $70 \mu\text{m}$. The Ni hollow fiber heated in air was composed of nanowires parallel to the axis of the starting silk. The dielectric loss of the prepared Ni/silk fiber and Ni hollow fiber (heated in nitrogen) is high up to 1 even at 18 GHz. The values of the magnetic loss of those two kinds of fiber are about 0.1–0.2 in 2–18 GHz.

Acknowledgement

This work was financially supported by “The Science Fund for Distinguished Young Scholars of Henan Province, China” (Contract No. 0512002400).

References

- [1] M.Z. Wu, H.H. He, Z.S. Zhao, X. Yao, *J. Phys. D: Appl. Phys.* 34 (2001) 1069–1074.
- [2] M.Z. Wu, Z.S. Zhao, H.H. He, X. Yao, *J. Magn. Magn. Mater.* 217 (2000) 89–92.
- [3] M. Matsumoto, Y. Miyata, *IEEE Trans. Magn.* 33 (1997) 4459–4464.
- [4] P. Chen, R.X. Wu, T.E. Zhao, F. Yang, Q. John, *J. Phys. D: Appl. Phys.* 38 (2005) 2302–2305.
- [5] I.T.H. Chang, Z. Ren, *Mater. Sci. Eng. A* 375–377 (1/2 (special issue)) (2004) 66–71.
- [6] Ph. Toneguzzo, G. Viau, O. Acher, F. Guillet, E. Bruneton, F. Fievet-Vincent, F. Fievet, *J. Mater. Sci.* 35 (2000) 3767–3784.
- [7] R.C. Che, Y.Q. Li, Z.H. Chen, H.J. Lin, *J. Mater. Sci. Lett.* 18 (1999) 1963–1964.
- [8] D.L. Griscom, J.J. Krebs, A. Perez, M. Treilleux, *Nucl. Instrum. Methods Phys. Res., Sect. B: Beam Interact. Mater. Atoms* B32 (1988) 272–278.
- [9] R.D. Bruyne, *Adv. Mater. Processes* 147 (1995) 33.
- [10] P. Rudkowski, G. Rudkowska, *J. Appl. Phys.* 69 (1991) 5017.
- [11] P. Rudkowski, G. Rudkowska, A. Zaluska, J. Strom-Olsen, *IEEE Trans. Magn.* 28 (1992) 1899.
- [12] J. Strom-Olsen, *Mater. Sci. Eng. A* 178 (1994) 239.
- [13] G. Liu, *Rare Met. Mater. Eng.* 23 (1994) 7.
- [14] F.Z. Kong, X.B. Zhang, W.Q. Xiong, F. Liu, W.Z. Huang, Y.L. Sun, J.P. Tu, X.W. Chen, *Surf. Coat. Technol.* 155 (2002) 33–36.
- [15] H.P. Liu, G.A. Cheng, R.T. Zheng, Y. Zhao, *J. Mol. Catal. A: Chem.* 225 (2005) 233–237.
- [16] Y.J. Chen, M.S. Cao, Q. Xu, J. Zhu, *Surf. Coat. Technol.* 172 (2003) 90–94.
- [17] Q.Y. Zhang, M. Wu, W. Zhao, *Surf. Coat. Technol.* 192 (2005) 213–219.
- [18] S. Shukla, S. Seal, Z. Rahaman, K. Scammon, *Mater. Lett.* 57 (2002) 151–156.
- [19] A.X. Zeng, W.H. Xiong, J. Xu, *Mater. Lett.* 59 (2005) 524–528.
- [20] T. Kobayashi, J. Ishibashi, S. Mononobe, M. Ohtsu, H. Honma, *J. Electrochem. Soc.* 147 (2000) 1046.
- [21] L.M. Ang, T.S.A. Hor, C.Q. Xu, C.H. Tung, S.P. Zhao, J.L.S. Wang, *Carbon* 38 (2000) 363.
- [22] W.S. Chung, S.Y. Chang, S.J. Lin, *Plat. Surf. Finish.* 83 (1996) 68.
- [23] S. Schaeffers, L. Ras, A. Stanishevsky, *Mater. Lett.* 60 (2006) 706–709.
- [24] I.S. Kim, S.K. Lee, *Scripta Mater.* 52 (2005) 1045–1049.
- [25] W.B. Weir, *Proc. IEEE* 62 (1974) 33–36.
- [26] E.J. Vanzura, J.R. Baker-Jarvis, J.H. Grosvenor, *IEEE Trans. Microwave Theory Tech.* 42 (1994) 2063–2070.
- [27] G. Viau, F. Ravel, O. Acher, et al., *J. Appl. Phys.* 76 (1994) 6570–6572.